Journal of Solid State Chemistry 233 (2016) 205–210

Contents lists available at ScienceDirect

Journal of Solid State Chemistry

journal homepage: www.elsevier.com/locate/jssc

The exchange interactions and the state of manganese atoms in the solid solutions in Bi_3NbO_7 of cubic and tetragonal modifications

N.V. Chezhina [a,*], N.A. Zhuk [b], D.A. Korolev [a]

[a] St. Petersburg State University, Universitetskii pr. 26, St. Petersburg 198504, Russia
[b] Syktyvkar State University, Oktyabr'skii pr. 55, Syktyvkar, Komi Republic 167001, Russia

ARTICLE INFO

Article history:
Received 11 September 2015
Received in revised form
9 October 2015
Accepted 10 October 2015
Available online 20 October 2015

Keywords:
Bismuth niobate
Fluorite-type structure
Magnetic properties
Exchange interactions

ABSTRACT

The comparative analysis of magnetic behavior of manganese-containing solid solutions $Bi_3Nb_{1-x}Mn_xO_{7-\delta}$ ($x=0.01-0.10$) of cubic and tetragonal modifications was performed. Based on the results of magnetic susceptibility studies paramagnetic manganese atoms in solid solutions of cubic and tetragonal modifications were found to be in the form of Mn(III), Mn(IV) monomers and exchange-coupled dimers of Mn(III)–O–Mn(III), Mn(IV)–O–Mn(IV), Mn(III)–O–Mn(IV). The exchange parameters and the distribution of monomers and dimers in solid solutions as a function of the content of paramagnetic atoms were calculated.

1. Introduction

Solid electrolytes on the basis of bismuth oxide have a high oxygen conductivity and are promising as materials for fuel cells, oxygen sensors and oxygen-conducting membranes of catalytic reactors [1–3]. Ionic conductivity, necessary for practical application, in a cubic high-temperature phase of bismuth oxide (δ-Bi_2O_3) is reached at 730 °C and is equal to 1.0 S/cm [4]. The area of practical application of δ-Bi_2O_3 is limited by a narrow temperature interval of its thermodynamic stability (730–825 °C) [5]. It is possible to stabilize δ-Bi_2O_3 by partial iso- and heterovalent replacement of bismuth atoms by atoms of transition elements (Y, Nb, Ta, W) or lanthanides (Gd, Er) [6–10]. It is found [11,12] that such solid solutions show mixed electronic and ionic conductivity and are promising for use in electrochemical devices.

In the binary Bi_2O_3–Nb_2O_5 system upon the mole ratio of bismuth to niobium $1.0 \le n(Bi)/n(Nb) \le 5.3$ the formation of four types of crystal structures derivative from fluorite structure were found [13,14]. Bismuth niobate Bi_3NbO_7 has two polymorphic modifications – tetragonal (type III) and cubic (type II) [14]. The tetragonal phase is formed in the temperature range from 800 to 900 °C and is stable on cooling to room temperature. Beyond this temperature range (> 750 °C) bismuth niobate crystallizes in cubic syngony [14,15]. The phase transition from tetragonal structure to cubic structure was found earlier to be reversible [16].

Cubic bismuth niobate has a defect fluorite-type structure (S.G. *Fm*3*m*), the unit cell parameter is $a=0.548$ nm. The atoms of Bi(III) and Nb(V) are in the same system of crystal sites [8]. Niobium atoms are located in distorted octahedra of oxygen atoms [9,14]. As a result of examining the crystal structure of bismuth niobate and its solid solutions by the methods of neutron and electron diffraction niobium atoms were found to be distributed in the lattice in a non-statistic manner [9,10,14–21]. Niobium–oxygen octahedra are combined in chains and blocks via oxygen atoms. Layered structure of the tetragonal phase of bismuth niobate $Bi_{94}Nb_{32}O_{221}$ (*I*-4*m*2, $a=1.6380$ nm, $c=3.8542$ nm) is a hybrid of fluorite and pyrochlore structures, niobium–oxygen octahedra being combined by oxygen atoms into chains and tetrahedra, those latter being the structural fragments of pyrochlore structure [9,15,16].

Bismuth niobate has a lower conductivity than δ-Bi_2O_3 owing to a decrease in the fraction of oxygen vacancies [4,5]. Heterovalent substitution of 3*d*-element atoms, of Zr, Y, W, Er for niobium atoms results in an increase in conductivity [17–21]. The nature of the current carriers and the mechanism of conductivity of bismuth niobate are studied in [22,23]. The conductivity in bismuth niobate was shown to be electron-ionic rather than purely ionic, the electron-ionic conductivity is ascribed to the presence of a small fraction of Nb(IV) ions located in the chains of niobium–oxygen octahedra.

Recently the interest to bismuth niobate and solid solutions on its basis increased markedly in the context of the discovery of its photocatalytic activity in the UV and visual diapason of the

* Corresponding author.
E-mail address: chezhina@nc2490.spb.edu (N.V. Chezhina).

http://dx.doi.org/10.1016/j.jssc.2015.10.026
0022-4596/

spectrum [24,25].

As a result of our earlier studies of magnetic properties of cubic $Bi_3Nb_{1-x}Ni_xO_{7-\delta}$ nickel atoms in the solid solutions were found to be as Ni(II) and predominantly as low spin Ni(III) because of the charge unbalance resulting from heterovalent substitution and from a strong distortion of the octahedral surrounding of paramagnetic atoms [26]. The structure is stabilized at the expense of formation of clusters of Ni(III) with antiferromagnetic superexchange. Its realization is possible owing to an aggregation of niobium–oxygen octahedral sites in the structure.

Nickel containing solid solutions are known only for high temperature cubic modification and are formed in a narrow concentration range, hence it appears impossible to analyze the influence of special features of the crystal structure and the nature of transition element atoms on the properties of solid solutions of cubic and tetragonal modification. Moreover, it is noted in [22,27] that the unit cell parameter of cubic bismuth niobate and solid solutions on its basis depends on the temperature of synthesis, which is associated with a redistribution of oxygen atoms in the anion sublattice and, as a consequence, a change in the total conductivity of the samples.

The solid solutions based on bismuth niobate and containing manganese appear to be stable in both modifications and over rather a wide range of concentrations. This is promising from the point of view of examining the chemical structure of both phases, of revealing the influence of the phase transition on the interatomic interactions. Therefore the aim of this work is to study magnetic properties of bismuth niobate and $Bi_3Nb_{1-x}Mn_xO_{7-\delta}$ solid solutions. An important special feature of our study was that cubic phases of pure bismuth niobate and of the solid solutions were obtained by sintering the tetragonal phase at the temperatures higher than the temperature of the phase transition.

2. Experimental

We synthesized Bi_3NbO_7 and the $Bi_3Nb_{1-x}Mn_xO_{7-\delta}$ solid solutions ($x=0.01$–0.10) by ceramic procedure from special pure grade Bi_2O_3 (99.998%), Nb_2O_5 (99.990%), and Mn_2O_3 (99.995%) oxides. Thoroughly ground oxide mixtures were pressed into pellets and sintered successively at 750, 850, 1000 °C for 40 h at each temperature, they were quenched in air. Thus at 750 °C and 1000 °C we obtained the samples of cubic modification and at 850 °C the samples of tetragonal modification resulted. The obtained samples were single phase, which was attested by the methods of X-ray analysis (a DRON-4-13 diffractometer, Cu$K\alpha$ emission) (Fig. 1) and electron scanning microscopy (a spectrometer of LINK firm). The unit cell parameters were calculated using the CSD program package [28].

The quantitative analysis of the fractions of metal cations in the samples was carried out by the method of atom-emission spectroscopy (a SPECTRO CIROS ISP spectrometer). The accuracy of relative measurements was 5%.

The magnetic susceptibility of the samples of cubic and tetragonal modifications was measured by Faraday method in the temperature range 77–400 K at 16 fixed temperatures and at the magnetic field strength 7240, 6330, 5230, and 3640 Oe. A semicommercial installation created in the laboratory of magnetochemistry of St. Petersburg State University and consisting of an electromagnet, an electronic balance, and a cryostate was used for magnetic susceptibility measurements. The accuracy of relative measurements – 1%. Diamagnetic corrections for calculations of paramagnetic component of magnetic susceptibility (χ_{Mn}^{para}, emu/mol) were introduced with respect to the susceptibility diamagnetic matrices of both modifications measured over the same temperature range.

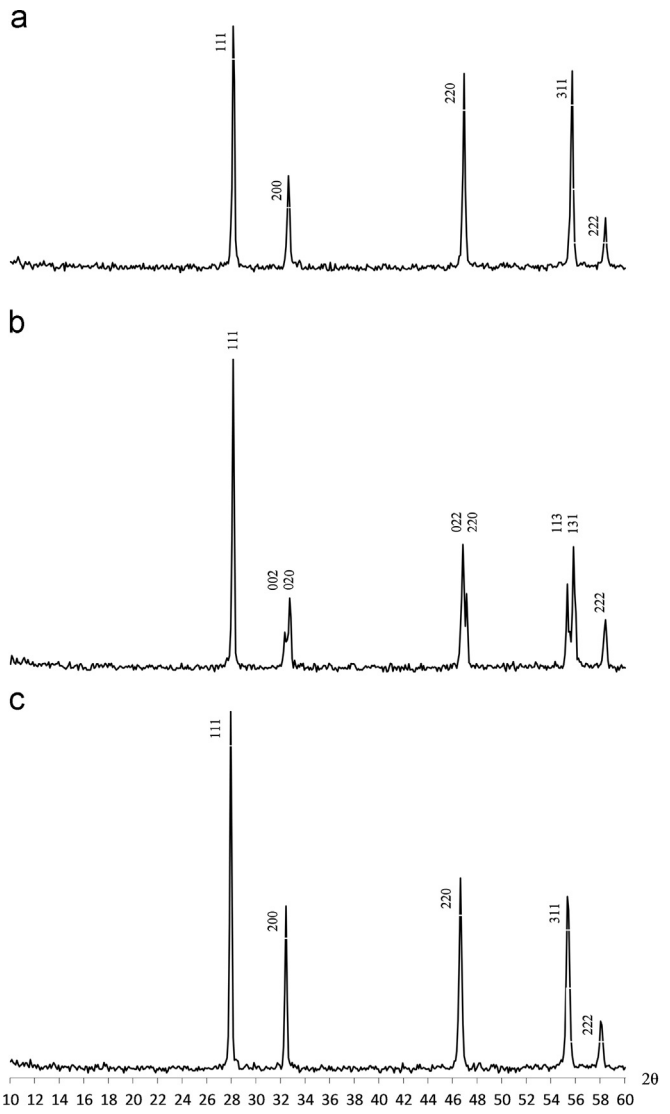

Fig. 1. (a, b, c) X-ray patterns for bismuth niobate of various modifications: (a) low-temperature cubic; (b) tetragonal; (c) high-temperature cubic.

3. Results and discussion

We studied the magnetic susceptibility of pure bismuth niobate of cubic and tetragonal modifications. Magnetic susceptibility of both samples being diamagnetic moderately depends on temperature, which could be expected since it is impossible to obtain absolutely pure compounds. However the susceptibility of tetragonal modification exceeds the susceptibility of cubic modification at low temperatures and has a more pronounced dependence on temperature. We believe this to be due to the presence of a fraction of Nb(IV) in both phases, its quantity being greater in tetragonal bismuth niobate. A decrease in its quantity in the cubic phase seems to be associated with oxidation of Nb(IV) to Nb (V) during high temperature sintering. An approximate estimation of the mole fraction of Nb(IV) in the tetragonal phase showed that its content exceeds the fraction of Nb(IV) in the cubic phase by 0.38%, moreover these atoms are bound within the tetrahedral niobium octahedral clusters by antiferromagnetic superexchange interactions [29]. Such a small content of Nb(IV) in the tetragonal phase must not have a substantial impact on electrophysical properties [23].

The $Bi_3Nb_{1-x}Mn_xO_{7-\delta}$ solid solutions are obtained in a rather wide concentration range, up to $x=0.10$. The unit cell parameter of

cubic solid solutions moderately decreases as the content of manganese atoms increases from $a=0.5475$ nm ($x=0.005$) to 0.5462 nm ($x=0.08$), which seems to be associated with isomorphous substitution of manganese atoms in the octahedra for niobium atoms close in their sizes – $r_{Nb(V)}=0.064$ nm; $r_{Mn(III)}=0.0645$ nm, $r_{Mn(IV)}=0.053$ nm [30]. For tetragonal solid solutions parameter a remains almost unchanged (at the average 0.5473 nm), parameter c slightly decreases from 0.5563 to 0.5542 nm.

We found that the dependencies of the inverse paramagnetic component on temperature ($1/\chi_{Mn}$–T) are linear, i.e. the susceptibilities obey Curie–Weiss law over the whole temperature range under study. Weiss constant is negative, which points to antiferromagnetic exchange interactions since the ground states of manganese atoms in any stable valence state are either singlet or dublet (Mn(II) $^6A_{1g}$; Mn(III) ^5E_g; Mn(IV) $^4A_{2g}$), which means that the effective magnetic moment of single atoms does not depend on temperature, and Weiss constant may be associated only with exchange interactions. The isotherms of magnetic susceptibility [χ_{Mn}^{para}–x] for the solid solutions of cubic and tetragonal modifications are given in Fig. 2. They are typical for the dilution of antiferromagnets. As is seen from Table 1, the paramagnetic susceptibilities for cubic samples synthesized at 1023 and 1223 K are almost identical, which points to the same electron state of manganese atoms and superexchange interactions between them. Since magnetic characteristics of the solid solutions are extremely sensitive to the distortions of polyhedral surrounding, to the bond parameters of paramagnetic atoms, the identity of magnetic characteristics of the solid solutions testifies to the identity of crystal structures of both cubic phases.

A comparison between the isotherms of magnetic susceptibility of cubic and tetragonal solid solutions shows (Fig. 2) that tetragonal solid solutions are characterized by lower magnetic susceptibilities over the whole concentration range, though are also typical for the dilution of antiferromagnets. Taking into account the fact that tetragonal solid solutions are obtained from the solid solutions of cubic (low temperature) modification at the temperature elevated by 100 K, the changes in the magnetic susceptibility must be assigned to the special features of manganese atom distribution and exchange interactions determined by the structure of tetragonal phase.

The effective magnetic moments calculated from concentration dependencies of χ_{Mn}^{para} to the infinite dilution ($\mu_{eff}^{x\to 0}$) for the solid solutions of both modifications depend on temperature and are given in Table 2. The values of the effective magnetic moments and their temperature dependence point to the presence of clusters of manganese atoms even at $x\to 0$ with antiferromagnetic superexchange between them. They can be Mn(III)–O–Mn(III) and Mn(IV)–O–Mn(IV). Single Mn(III) and Mn(IV) atoms can also exist as well as their ferromagnetically coupled dimmers Mn(III)–O–Mn(IV).

As the concentration of manganese atoms increases, the dependence of magnetic moments on temperature becomes more distinct, which points to the development of antiferromagnetic exchange (Fig. 3). The run of temperature dependencies of μ_{eff} in the tetragonal solid solutions have engaged our attention: up to $x=0.04$ μ_{eff} is almost the same at low temperatures, which may be determined by an approximately equal fraction of single manganese atoms (monomers), their magnetic moment being independent on temperature.

As is noted in [31] the electron spin resonance (ESR) spectra of

Table 1
Comparison between the paramagnetic components of magnetic susceptibilities of low-temperature (1073 K) and high-temperature (1273 K) cubic solid solutions.

x	Temperature of synthesis, K	χ_{Mn}^{para}, emu/mol		
		90 K	180 K	240 K
0.014	1073	0.0116	0.0065	0.0048
	1273	0.0115	0.0065	0.0050
0.020	1073	0.0118	0.0064	0.0049
	1273	0.0120	0.0067	0.0052
0.048	1073	0.0096	0.0054	0.0042
	1273	0.0105	0.0058	0.0045
0.061	1073	0.0104	0.0055	0.0042
	1273	0.0103	0.0054	0.0041

Table 2
The effective magnetic moments of manganese atoms in $Bi_3Nb_{1-x}Mn_xO_{7-\delta}$ of cubic (μ_1) and tetragonal (μ_2) modifications at $x\to 0$.

T, K	90	120	180	240
μ_1, μB	3.54	3.69	3.91	4.01
μ_2, μB	2.76	2.97	3.25	3.42

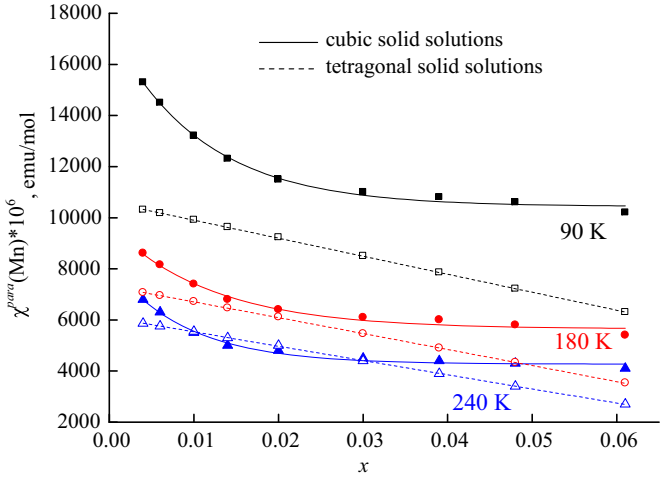

Fig. 2. Plots of paramagnetic components of magnetic susceptibility of the $Bi_3Nb_{1-x}Mn_xO_{7-\delta}$ solid solutions vs manganese content x for various temperatures.

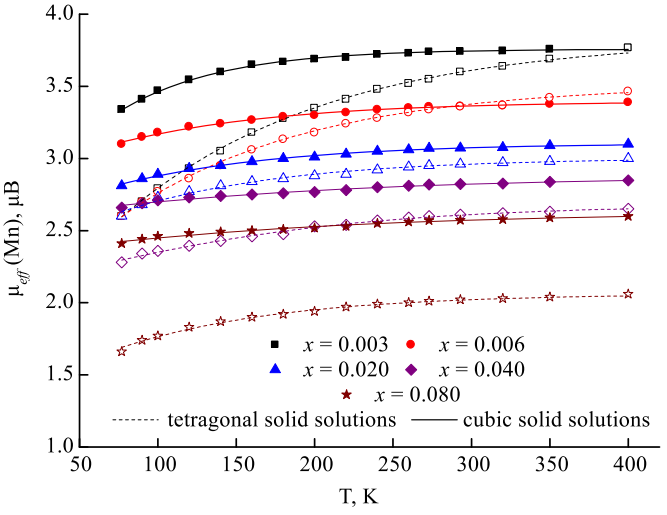

Fig. 3. Temperature dependencies of the effective magnetic moments in the cubic and tetragonal solid solutions with various concentrations of manganese.

the solid solutions under study with $x=0.005$ and 0.03 of cubic and tetragonal modification obtained at 850 and 950 °C (recorded with the help of a SE/X-2547, RadioPAN) are similar. There is only a broad line with $g\sim 3.47$, which is not typical for Mn(II) or Mn(IV). The identity of ESR spectra for both modifications can point to the same electron states of manganese atoms.

With the aim of describing the experimental dependencies of χ_{Mn}^{para}–x for both kinds of solid solutions we carried out the theoretical calculation of magnetic susceptibility.

The calculation was performed within the framework of the diluted solid solution model [32]. Magnetic susceptibility is determined as a sum of contributions of single paramagnetic atoms (monomers) and of their various clusters. For diluted solutions such clusters may be taken as dimers (M–O–M). In our case the monomers may be Mn(III) and Mn(IV), and the dimers are Mn(III)–O–Mn(III), Mn(IV)–O–Mn(IV) and Mn(III)–O–Mn(IV). With regard to the above said the formula for calculating the paramagnetic component of magnetic susceptibility is the following:

$$\chi_{calc}^{para}(Mn) = a_{Mn(III)-Mn(III)}^{dim}\chi_{Mn(III)-Mn(III)}^{dim} + a_{Mn(III)}^{mon}\chi_{Mn(III)}^{mon} + a_{Mn(IV)-Mn(IV)}^{dim}\chi_{Mn(IV)-Mn(IV)}^{dim} + a_{Mn(III)-Mn(IV)}^{dim}\chi_{Mn(III)-Mn(IV)}^{dim} + (1 - a_{Mn(III)-Mn(III)}^{dim} - a_{Mn(III)}^{mon} - a_{Mn(IV)-Mn(IV)}^{dim} - a_{Mn(III)-Mn(IV)}^{dim})\chi_{Mn(IV)}^{mon} \quad (1)$$

Here $a_{Mn(III)}^{mon}$ – the fraction of Mn(III) atoms; $a_{Mn(III)-Mn(III)}^{dim}$, $a_{Mn(IV)-Mn(IV)}^{dim}$, $a_{Mn(IV)-Mn(III)}^{dim}$ – the fractions of dimers of Mn(III) and Mn(IV) atoms; $\chi_{Mn(III)-Mn(III)}^{dim}$, $\chi_{Mn(IV)-Mn(IV)}^{dim}$, $\chi_{Mn(III)-Mn(IV)}^{dim}$, $\chi_{Mn(III)}^{mon}$, $\chi_{Mn(IV)}^{mon}$ magnetic susceptibilities of Mn(III)–O–Mn(III), Mn(IV)–O–Mn(IV), Mn(III)–O–Mn(IV) dimers, and Mn(III) and Mn(IV) monomers respectively.

Formula (2) contains seven independent parameters: the fractions of single Mn(III) and Mn(IV) atoms, the fraction of various dimers, and the parameters of antiferromagnetic exchange between manganese atoms in the same valence state and ferromagnetic exchange $J_{Mn(III)-Mn(IV)}$. The number of experimental values of magnetic susceptibility (the number of concentrations and 16 temperature points for each x) is sufficient for confident estimation of the exchange parameters and fractions of various clusters, as has been shown before [33–38].

According to Heisenberg–Dirac–Van–Vleck model [39], magnetic susceptibility of dimer clusters of paramagnetic atoms can be calculated by formula (3):

$$\chi_{dim}^{S_1-S_2} = \frac{g^2}{16T}\frac{\sum_{S'} S'(S'+1)(2S'+1)e^{-\frac{E(J,S)}{kT}}}{\sum_{S'}(2S'+1)e^{-\frac{E(J,S)}{kT}}} \quad (2),)$$

where S_1, S_2 – atom spins in the dimer; g – g-factor for Mn(III) and Mn(IV); J the exchange parameter; energy of spin levels $E(J, S') = -J[S'(S'+1) - S_1(S_1+1) - S_2(S_2+1)]$; the total spin $S' = S_1 + S_2,\ S_1 + S_2 - 1,\ \ldots,\ |S_1 - S_2|$.

The agreement between calculated and experimental values is achieved upon minimizing the $\sum_i \sum_j (\chi_{ij}^{calc} - \chi^{exp})^2$ function, where i means summing up by all the concentrations; j-summing up by all the temperatures, χ_{ij}^{calc}, χ_{ij}^{exp}– calculated and experimental values of paramagnetic component of magnetic susceptibility of the solid solutions under study.

The best agreement between experimental and calculated data for cubic solid solutions was obtained for $J_{Mn(III)-Mn(III)} = -170\ cm^{-1}$, $J_{Mn(IV)-Mn(IV)} = -23\ cm^{-1}$, $J_{Mn(III)-Mn(IV)} = +40\ cm^{-1}$. For tetragonal modification the exchange parameters were $J_{Mn(III)-Mn(III)} = -135\ cm^{-1}$, $J_{Mn(IV)-Mn(IV)} = -20\ cm^{-1}$, $J_{Mn(III)-Mn(IV)} = +65\ cm^{-1}$. The correlation

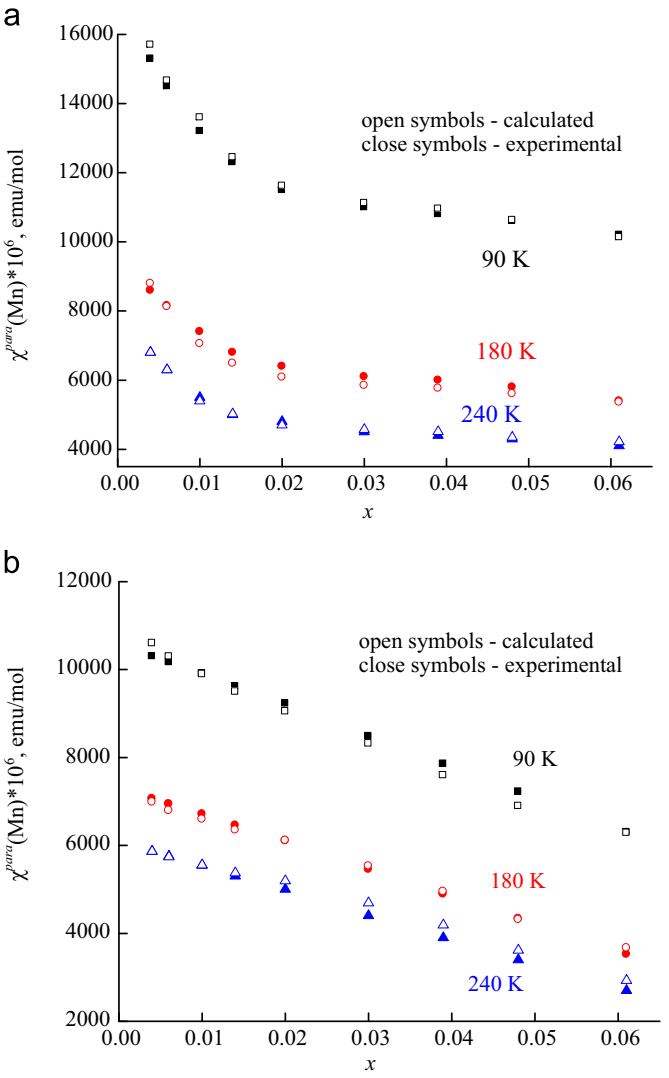

Fig. 4. (a, b) A comparison between calculated (open symbols) and experimental (close symbols) paramagnetic components of magnetic susceptibility for (a) cubic and (b) tetragonal solid solutions.

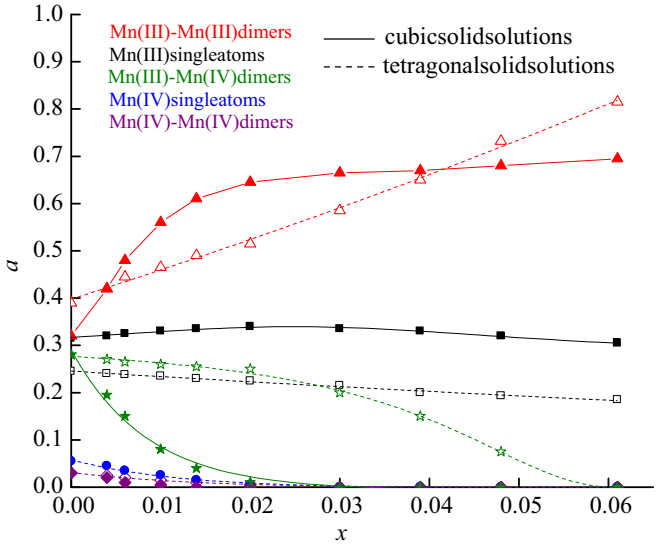

Fig. 5. The dependencies of cluster fractions and single atoms vs concentration of manganese for cubic and tetragonal solid solutions.

between experimental and calculated magnetic susceptibilities is given in Fig. 4(a,b).

The results of our calculations showed that in the infinitely diluted cubic solid solution there are single Mn(III) and Mn(IV) atoms and their dimers with antiferromagnetic and ferromagnetic type of exchange (Fig. 5). The induced oxidation of Mn(III) to Mn (IV) partially levels the effect of the charge unbalance resulting from heterovalent substitution for niobium atoms, which was noted earlier in [33–38]. As the concentration of manganese increases the fraction of oxidated Mn(IV) atoms as monomers and dimers substantially decreases, which at first glance seems to be contradictory: the number of oxygen vacancies due to Mn(III) increases and destabilizes the structure. We may suggest that in this case the structure is stabilized at the expense of exchange bound clusters of manganese atoms, which are more rigid than for nickel atoms [26]. Moreover, there is no signals of Mn(II) and Mn(IV) in the ESR spectra.

The exchange between Mn(III) atoms located in the diagonals of the unit cell faces is predominantly antiferromagnetic and is effected by the exchange channels $d_{x^2-y^2}\|p_x\|d_{x^2-y^2}$, $d_{xz}\|p_x\|d_{xz}$, $d_{xy}\|p_y\|d_{xy}$ and $d_{xz}\|p_z\|d_{xz}$.

Ferromagnetic exchange in the Mn(III)–O–Mn(IV) dimers is effected by the channels $d_{xy}\|p_y\perp p_z\|d_{xz}$, $d_{xy}\|p_x\perp p_z\|d_{xz}$. Such a conclusion agrees with the assumption about clustering of niobium–oxygen octahedra advanced as the result of examining the superstructure in cubic and tetragonal bismuth niobate and in the solid solutions [3,8,9,17–21]. The formation of dimers rather than more complex clusters or chains of paramagnetic atoms seems to be associated with a low concentration of paramagnetic atoms in the solid solutions under study.

Antiferromagnetic exchange interactions result from overlapping of the orbitals of paramagnetic atoms with oxygen orbitals. An increase in the absolute value of the exchange parameter for Mn(III) atoms in comparison with Ni(III) atoms [26] must be due to unpaired electrons in d_{xy}, d_{xz}, d_{yz} orbitals of Mn(III).

In the solid solutions of tetragonal modification as distinct from cubic modification the antiferromagnetic exchange is weaker ($J_{\mathrm{Mn(III)–Mn(III)}}=-135\ \mathrm{cm}^{-1}$, $J_{\mathrm{Mn(IV)–Mn(IV)}}=-20\ \mathrm{cm}^{-1}$) and ferromagnetic exchange, which is not associated with overlapping is stronger ($J_{\mathrm{Mn(III)–Mn(IV)}}=65\ \mathrm{cm}^{-1}$). This difference in the magnetic behavior seems to be determined by different joining of niobium–oxygen octahedra in the structure and by the changes in the angle and the bond length between Nb(Mn)–O–Nb(Mn) atoms. The distortions of coordination polyhedra due to oxygen vacancies resulting from the substitution of Mn(III) for Nb(V) affect the M–O–M bond angle, and in the tetragonal modification it appears to deviate from 180° to a greater extent than in the cubic modification, which decreases the overlapping of $d_{x^2-y^2}$ orbitals with corresponding p-orbitals of oxygen atoms and also p_π–d_π-overlapping. This in its turn decreases the absolute value of antiferromagnetic exchange parameter and increases the ferromagnetic exchange parameter from $+40$ to $+65\ \mathrm{cm}^{-1}$. We emphasize that the direct overlapping of $d_{x^2-y^2}$orbitals with $p_x(p_y)$-orbitals of oxygen is responsible for the greatest contribution to the antiferromafnetic superexchange, therefore the deviation of the angle Mn–O–Mn from 180° results in the most significant effect on exchange parameter.

We should concentrate our attention on the fact that in the tetragonal structure in the infinitely diluted solution the fraction of dimers of paramagnetic atoms is greater than in the cubic structure, and their number increases more rapidly as the concentration increases (Fig. 5). This can be accounted for by assuming that aggregation of paramagnetic atoms first occurs in octahedral clusters, which are present from the outset in the tetragonal structure. This means that the rigidity of the aggregates of paramagnetic atoms is determined by other interactions associated with the bond energy rather than by the exchange.

4. Conclusions

The reversible phase transition low-temperature cubic ↔ tetragonal ↔ high-temperature cubic modifications of the $Bi_3Nb_{1-x}Mn_xO_{7-\delta}$ solid solutions results in a decrease in strength of antiferromagnetic superexchange on passing from cubic to tetragonal phase, at the same time the fractions of clusters of manganese atoms increases. Both cubic modifications have the same magnetic characteristics, thus the same states of manganese atoms and the degree of clustering. These results are the more interesting that various modifications were obtained from the same low-temperature cubic phase.

Acknowledgments

The authors express their gratitude to V. Lutoev (Institute of Geology, Komi Sci Center, Ural branch of Russian Acad. Sci., Syktyvkar) for recording the ESR spectra.

References

[1] T. Takahashi, H. Iwahara, T. Esaka, J. Appl. Electrochem. 7 (1977) 303–308.
[2] K.Z. Fung, J. Chen, A.V. Virkar, J .Am. Ceram. Soc. 76 (1993) 2403–2418.
[3] M. Struzik, X. Liu, I. Abrahams, F. Krok, M. Malys, J.R. Dygas, Solid State Ion. 218 (2012) 25–30.
[4] T. Takahashi, H. Iwahara, Y. Nagaj, J. Appl. Electrochem. 2 (1972) 97–104.
[5] H.A. Harwig, A.G. Gerards, J. Solid State Chem. 26 (1978) 265–274.
[6] P. Shuk, H.D. Wiemhofer, U. Guth, M. Gopel, Solid State Ion. 89 (1996) 179–196.
[7] A. Castro, E. Aguado, J.M. Rojo, P. Herrero, R. Enjalbert, J. Galy, Mater. Res. Bull. 33 (1998) 31–41.
[8] W. Zhou, J. Solid State Chem. 108 (1994) 381–394.
[9] C.D. Ling, J. Solid State Chem. 148 (1999) 380–405.
[10] A.A. Yaremchenko, V.V. Kharton, E.N. Naumovich, A.A. Vecher, J. Solid State Electrochem. 2 (1998) 146–149.
[11] A. Castro, D. Palem, J. Mater. Chem. 12 (2002) 2774–2780.
[12] D. Hirabayashi, A. Hashimoto, T. Hibino, U. Harada, M. Sano, Electrochem. Solid State Lett. 7 (2004) 108–110.
[13] W. Zhou, D.A. Jefferson, J.M. Thomas, J. Solid State Chem. 70 (1987) 129–136.
[14] C.D. Ling, R.L. Withers, S.S. Schmid, J.G. Thompson, J. Solid State Chem., 119, (1998) 42–61.
[15] C.D. Ling, M.A. Johnson, J. Solid State Chem. 177 (2004) 1838–1846.
[16] N.A. Zhuk, N.V. Rozhkina, Russ. J. Gen. Chem. 84 (2014) 1–5.
[17] D. Tang, W. Zhou, J. Solid State Chem. 119 (1995) 311–318.
[18] I. Abrahams, F. Krok, W. Wrobel, A. Kozanecka-Szmigiel, S.C.M. Cham, Solid State Ion. 179 (2008) 2–8.
[19] I. Abrahams, F. Krok, A. Kozanecka-Szmigiel, S.C.M. Cham, J.R. Dygas, J. Power Sour. 173 (2007) 788–794.
[20] I. Abrahams, F. Krok, S.C.M. Cham, W. Wrobel, A. Kozanecka-Szmigiel, A. Luma, J.R. Dygas, J. Solid Electrochem. 10 (2006) 569–574.
[21] M. Leszczynska, M. Holdynski, F. Krok, I. Abrahams, X. Liu, W. Wrobel, Solid State Ion. 181 (2010) 796–811.
[22] X.P. Wang, G. Corbel, S. Kodjikian, Q.F. Fang, P. Lacorre, J. Solid State Chem. 179 (2006) 3338–3346.
[23] M. Malys, M. Holdynski, F. Krok, W. Wrobel, J.R. Dygas, C. Pirovano, R. N. Vannir, E. Capoen, I. Abrahams, J. Power Sour. 194 (2009) 16–19.
[24] J. Fang, J. Ma, Y. Sun, Z. Liu, C. Gao, Solid State Sci. 13 (2011) 1649–1653.
[25] W. Wu, S. Liang, L. Shen, Z. Ding, H. Zheng, W. Su, L. Wu, J. Alloy. Compd. 520 (2012) 213–219.
[26] N.V. Chezhina, N.A. Zhuk, V.N. Zharenkova, V.P. Lyutoev, Russ. J. Gen. Chem. 85 (2015) 521–526.
[27] M. Valant, D. Suvorov, J. Am. Ceram. Soc. 86 (2003) 939–944.
[28] L.G. Akselrud, Y.M. Gryn, P.Yu Zavalij, V.K. Pecharsky, V.S. Fundamensky, Coll. Abstr. XII Europ. Crystallogr. Meet., vol. III, USSR Academy Sci, Moscow (1989), p. 155.
[29] N.V. Chezhina, N.A. Zhuk, V.P. Lyutoev, Russ. J. Gen. Chem. 85 (2015) 1599–1601.
[30] R.D. Shannon, Acta Crystallogr. A 32 (1976) 751–767.
[31] N.A. Zhuk, E.S. Girut, T.A. Popova, T.V. Obedina, Proc. Komi sc. Ud. Ras. 17 (2014) 10–15 (in Russian).
[32] N.V. Chezhina, D.A. Korolev, Solid State Ion. 225 (2012) 201–205.
[33] N.A. Zhuk, I.V. Piir, N.V. Chezhina, Russ. J. Gen. Chem. 76 (2006) 1705–1709.

[34] N.A. Zhuk, I.V. Piir, N.V. Chezhina, Russ. J. Gen. Chem. 76 (2006) 1710–1715.
[35] N.A. Zhuk, I.V. Piir, N.V. Chezhina, Russ. J. Gen. Chem. 78 (2008) 376–382.
[36] N.A. Zhuk, I.V. Piir, N.V. Chezhina, Russ. J. Gen. Chem. 77 (2007) 215–220.
[37] N.V. Chezhina, I.V. Piir, N.A. Zhuk, Russ. J. Gen. Chem. 78 (2008) 1135–1138.
[38] N.V. Chezhina, I.V. Piir, N.A. Zhuk, Russ. J. Gen. Chem. 84 (2014) 185–189.
[39] V.T. Kalinnikov, Yu.V. Rakitin, Introduction to Magnetochemistry: The Static Magnetic Susceptibility Method in Chemistry, Nauka, Moscow, 1980 (in Russian).